

Triptolide is a traditional Chinese medicine-derived inhibitor of polycystic kidney disease

Stephanie J. Leuenroth*, Dayne Okuhara†, Joseph D. Shotwell*, Glen S. Markowitz‡, Zhiheng Yu†, Stefan Somlo†§, and Craig M. Crews*¶||**

Departments of *Molecular, Cellular, and Developmental Biology, †Internal Medicine, §Genetics, ¶Pharmacology, and ||Chemistry, Yale University, New Haven, CT 06511; and ‡Department of Pathology, College of Physicians and Surgeons, Columbia University, New York, NY 10027

Communicated by R. L. Erikson, Harvard University, Cambridge, MA, January 18, 2007 (received for review November 30, 2006)

During kidney organogenesis, tubular epithelial cells proliferate until a functional tubule is formed as sensed by cilia bending in response to fluid flow. This flow-induced ciliary mechanosensation opens the calcium (Ca^{2+}) channel polycystin-2 (PC2), resulting in a calcium flux-mediated cell cycle arrest. Loss or mutation of either PC2 or its regulatory protein polycystin-1 (PC1) results in autosomal dominant polycystic kidney disease (ADPKD), characterized by cyst formation and growth and often leading to renal failure and death. Here we show that triptolide, the active diterpene in the traditional Chinese medicine *Lei Gong Teng*, induces Ca^{2+} release by a PC2-dependent mechanism. Furthermore, in a murine model of ADPKD, triptolide arrests cellular proliferation and attenuates overall cyst formation by restoring Ca^{2+} signaling in these cells. We anticipate that small molecule induction of PC2-dependent calcium release is likely to be a valid therapeutic strategy for ADPKD.

ADPKD | calcium | natural product | polycystin | renal cyst

Autosomal dominant polycystic kidney disease (ADPKD) is the leading genetic cause of end-stage renal failure affecting between 1 in 500 and 1 in 1,000 live births (1). Mutations in the gene product of *PKD1*, polycystin-1 (PC1), account for ≈85% of all cases of ADPKD, with the remaining 15% being attributed to the transient receptor potential (TRP) Ca^{2+} channel polycystin-2 (PC2) (2, 3), the *PKD2* gene product (4). ADPKD cyst cells are characterized by somatic loss of the normal allele of the respective disease gene, resulting in increased cellular proliferation and, ultimately, the formation and growth of fluid-filled cysts. ADPKD patients who develop kidney failure require life-long renal function replacement by dialysis or kidney transplantation. It has been proposed that maintenance of normal tubule structure in the nephron is under the control of the mechanosensory function of the primary cilia, where both PC1 and PC2 colocalize (5–7). In response to luminal flow, the primary cilium bends and initiates a signaling cascade through the PC1/PC2 complex that activates signaling pathways required for maintaining nephron structure (5, 8). PC2 is hypothesized to work in complex with PC1 to mediate increases in cytosolic Ca^{2+} as part of its signal transduction (5). It is also believed that the disruption of a functional PC1/PC2 complex, through mutation or deletion, abolishes normal cellular Ca^{2+} signaling, thereby allowing for inappropriate proliferative signals (9–12). Recently, the immunosuppressant rapamycin and a vasopressin V2 receptor (VPV2R) antagonist have been shown to limit cyst progression in murine models of ADPKD by inhibition of PC1-mediated mTOR activation and decreasing intracellular cAMP levels, respectively (13–15). However, there is currently no therapeutic strategy to restore calcium release in ADPKD cystic kidney cells, which would slow the progression of ADPKD.

Work in our laboratory has previously focused on the mechanism of action of the potent, biologically active diterpene, triptolide (1) (Fig. 1A) (16). This natural product, isolated from the medicinal vine *Tripterygium wilfordii* Hook F (“Thunder God Vine”) and used in traditional Chinese medicine for centuries, has a myriad of therapeutic uses against cancer, inflammation, and autoimmune diseases (17–19). Triptolide has been shown to induce apoptosis or

cell growth arrest depending on its concentration and the cell type treated (16, 20–22). It is also a potent inhibitor of NF- κ B- and NF-AT-mediated transcription, and therefore leads to the down-regulation of many gene products necessary for the inflammatory response or cellular growth (23–25). We have additionally shown that triptolide’s mode of action can be differentiated by a calcium dependence because cell growth and cell death are sensitive to calcium concentrations, but transcriptional inhibition is not (16). Although studies on triptolide-mediated downstream signaling events have elucidated important biological findings, basic cellular interactions and potential binding proteins have not been identified. Our results here present an as of yet undescribed mechanism of action for triptolide and an ability to stimulate Ca^{2+} release, arrest cell growth, and reduce cyst progression in a model of ADPKD.

Results

PC2 Is a Putative Triptolide-Binding Protein. We have previously reported binding properties of [^3H]triptolide, including its predominant (noncovalent) interaction with the membrane fraction of the cell, an interaction with a high-molecular-weight protein or complex, and a requirement for intact cells to mediate binding activity (16). To continue with these studies, we sought to investigate triptolide’s mechanism of action through the identification of [^3H]triptolide-binding protein(s). Following extensive chromatographic protein fractionation, SDS/PAGE separation, MALDI-MS analysis, and Western blot confirmation, a potential 110-kDa [^3H]triptolide-binding protein was identified as PC2 (Fig. 1 B–D). Although we also identified other potential triptolide-binding proteins associated with the membrane-bound fraction of the cell, we began our studies focusing on PC2. We have previously demonstrated a Ca^{2+} dependence for triptolide-mediated apoptosis (high concentrations) and cytostatic activity (low concentrations), as well as a Ca^{2+} -mediated inhibition of [^3H]triptolide-binding activity (16). Given our previous results, we explored PC2 as a potential target for the biological activity of triptolide and tested its therapeutic efficacy in a model of ADPKD.

Murine Kidney Epithelial *Pkd2*^{−/−} Cells Are Less Sensitive to the Effects of Triptolide. To validate PC2 as a potential triptolide-binding protein and determine its importance in triptolide’s biological activity, we first examined triptolide-induced cell death as a function of PC2 expression (Fig. 2A). To do this, we used murine

Author contributions: S.J.L. and C.M.C. designed research; S.J.L., D.O., and J.D.S. performed research; Z.Y. contributed new reagents/analytic tools; S.J.L., D.O., G.S.M., S.S., and C.M.C. analyzed data; and S.J.L. and C.M.C. wrote the paper.

Conflict of interest statement: C.M.C. and S.S. are currently exploring the commercial implications of these findings and declare a potential conflict of interest.

Abbreviations: HBSS, Hank’s balanced salt solution; WBC, white blood cell; ADPKD, autosomal dominant polycystic kidney disease; SOC, store-operated channel; TRP, transient receptor potential; VPV2R, vasopressin V2 receptor.

*To whom correspondence should be addressed. E-mail: craig.crews@yale.edu.

This article contains supporting information online at www.pnas.org/cgi/content/full/0700499104/DC1.

© 2007 by The National Academy of Sciences of the USA

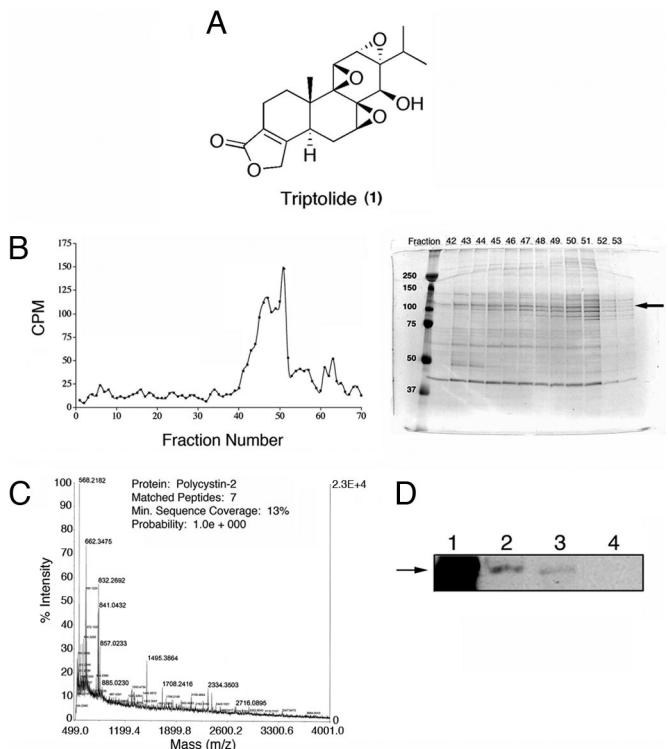


Fig. 1. Identification of PC2 as a protein associated with [³H]triptolide-binding activity. (A) Triptolide is a biologically active diterpene from the medicinal vine *Tripterygium wilfordii* Hook F. (B) [³H]triptolide-associated proteins were fractionated by FPLC over an increasing NaCl gradient. (*Left*) Fractions were tested for the presence of [³H]triptolide (cpm) and analyzed by SDS/PAGE. (*Right*) The Coomassie stained gel is shown; a main protein band at 110-kDa in fractions 43–51 (peak binding activity) is represented by the arrow. MW markers are on the left. (C) MALDI-MS analysis of 110-kDa band in *B* identified as PC2. (D) Western blot analysis with anti-PC2 antisera. Lane 1, positive control lysate; lane 2, purified sample before FPLC fractionation; lane 3, pooled fractions of [³H]triptolide positive samples; lane 4, pooled fractions of [³H]triptolide-negative samples.

kidney epithelial cell lines derived from *Pkd2*^{+/−} or *Pkd2*^{−/−} mice. All cell lines were assessed for normal PC2 expression as determined by indirect immunofluorescence and Western blot analysis (Fig. 2*B*). Following a 24-h incubation with 100 nM triptolide, PC2-expressing cells (*Pkd2*^{+/−}) underwent rapid cell death, whereas PC2-null cells (*Pkd2*^{−/−}) remained >90% viable (Fig. 2*A*). This effect was transient, however, because >50% of *Pkd2*^{−/−} cells were dead by a later 48-h time point (data not shown). To further reinforce the role of PC2 in triptolide's mechanism of action, stable expression of PC2 was reconstituted in *Pkd2*^{−/−} cells (*Pkd2*^{REX}) and assessed for triptolide-mediated cell death. Similar to the *Pkd2*^{+/−} line, >80% of *Pkd2*^{REX} cells died following a 24-h incubation with triptolide (Fig. 2*A*). Although these results implicate a role of PC2 in triptolide-mediated cell death, this effect was even more dramatic following 48 h with 25 nM triptolide (Fig. 2*A*). Although both the *Pkd2*^{+/−} and *Pkd2*^{REX} cell lines underwent cell death during this time course, *Pkd2*^{−/−} cells not only survived, but continued to grow (Fig. 2*A*), but at a slower rate as compared with untreated cells (Fig. 2*B*).

Triptolide has been previously shown to activate caspases (26, 27), therefore we investigated whether there was evidence for mitochondrial- or receptor-mediated caspase activation dependent upon PC2 expression. We assessed direct caspase activity of caspases-8, -9, and -3 at both 100 nM and 25 nM triptolide. Although weak activation of caspase-8 and -9 was initially detected, this activity could ultimately be eliminated upon addition of a

specific caspase-3 inhibitor during the assay (data not shown). Therefore, we focused only on caspase-3 activity preceding cell death in the absence or presence of PC2 expression. At 100 nM triptolide, caspase-3 activation in *Pkd2*^{−/−} cells was 50% less as compared with the *Pkd2*^{REX} cell line (Fig. 2*C*), thereby supporting our cell death results (Fig. 2*A*); 25 nM triptolide incubation for 18 h resulted in minimal caspase-3 activation in *Pkd2*^{−/−} cell lysates, as well as in an intact cellular assay (Fig. 2*C*). This supports our previous findings that a low concentration of triptolide (25 nM) is ineffective at causing global cell death in *Pkd2*^{−/−} cells. However, it is important to recognize that a secondary mechanism may be responsible for slowing of cell growth.

Triptolide Arrests Growth and Increases p21 Expression in *Pkd1*^{−/−} Kidney Cells. Because the majority of cases of ADPKD occur as a result of a mutation or loss of PC1, we next examined what effect triptolide would have on a murine kidney PC1-null cell line (*Pkd1*^{−/−}). Based upon our previous data in PC2-expressing cells (Fig. 2*A–C*), we expected that triptolide would also induce cell death in this line. Interestingly, although addition of 100 nM triptolide to *Pkd1*^{−/−} murine kidney epithelial cells caused minimal cell death, the majority of the cell population growth arrested and displayed a flattened morphology (Fig. 2*D*). In contrast, in the absence of triptolide, this cell line doubled in population approximately every 36 h as determined by cell viability assays (Fig. 2*D*). Additionally, PC2 expression was not altered in these cells because its staining pattern was consistent with ER localization (Fig. 2*D*). To further examine whether calcium was required for triptolide-mediated growth arrest (i.e., through a PC2-dependent mechanism), *Pkd1*^{−/−} cells were cultured in the absence or presence of Ca²⁺-containing media plus 100 nM triptolide. We first assessed normal growth rates and determined that cells grown in calcium-deficient media grew at approximately half the rate as compared with calcium-containing media (data not shown). After 72 h of continual culture with triptolide, cell growth was affected in both experimental conditions, although at different rates as compared with their respective controls (Fig. 2*E*). Cells grown in the presence of calcium showed their characteristic cell flattening, and no growth was observed over 3 days. In the absence of calcium, cell number increased beyond the initial seeding density; however, the growth rate was 3-fold less as compared with the untreated control. Although triptolide had the most pronounced effect on *Pkd1*^{−/−} cells in the presence of calcium, it should also be noted that multiple mechanisms possibly exist for the biological effects of triptolide on cell growth and viability.

Tissues that have lost PC1 expression have previously been shown to down-regulate p21^{CIP/WAF} (9). Therefore, we tested whether the proliferation inhibition we observed was associated with up-regulation of p21^{CIP/WAF} upon triptolide treatment. Over a 96-h time course, p21^{CIP/WAF} levels increased in triptolide-treated *Pkd1*^{−/−} cells, thus resulting in growth arrest. However, p53 protein levels remained unchanged (Fig. 2*F*). This is consistent with previous studies that implicate a p53-independent induction of p21^{CIP/WAF}, such as through the Jak/Stat pathway (9) or by the regulation of Id2 localization (10) in response to PC1 or PC2 activation. Interestingly, triptolide has previously been linked to conflicting reports in the literature of either decreased or up-regulated p21 expression depending on cell type and p53 status (20, 28, 29). It is therefore possible that p21 modulation resulting in cell death or cell growth arrest could also depend on PC1/ PC2 status as well as p53. Because these experiments provided evidence that triptolide-induced cell death or growth arrest could be modulated by PC2 expression, we next sought to determine whether triptolide could affect Ca²⁺ release.

Triptolide Causes Calcium Release Through a PC2-Dependent Pathway. To measure PC2-mediated Ca²⁺ release in response to triptolide, we used murine kidney epithelial cell lines differing in PC1 and PC2

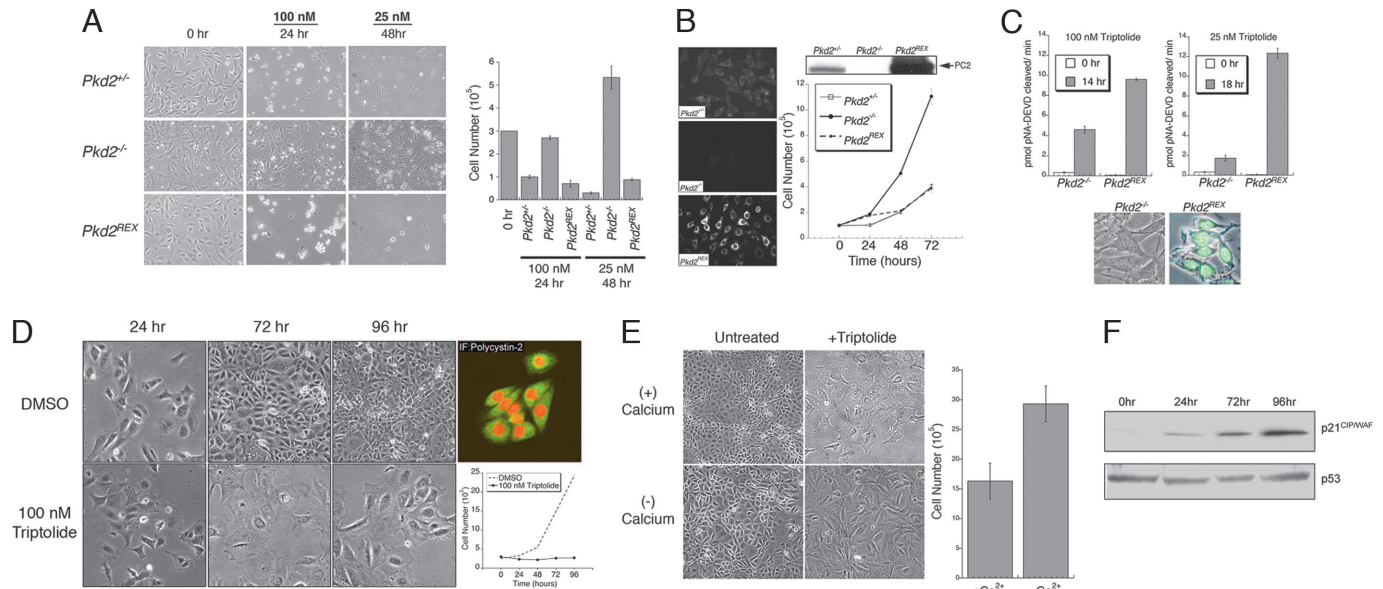


Fig. 2. PC2 expression is necessary for rapid cell death or growth inhibition induced by triptolide. (A) Murine kidney epithelial cells were plated at a starting density of 3×10^5 (0 h) and then treated with 100 nM triptolide for 24 h or 25 nM for 48 h. Cell viability was determined by trypan blue dye exclusion, and results are represented graphically ($n = 6$, mean \pm SE). (B) PC2 expression was assessed by indirect immunofluorescence (IF) detection and by Western blot analysis in each cell line ($Pkd2^{-/-}$, $Pkd2^{+/-}$, and $Pkd2^{REX}$). A normal growth curve is shown for a 72-h time course ($n = 3$, mean \pm SE). (C) Caspase-3 activity assays from $Pkd2^{-/-}$ and $Pkd2^{REX}$ cells treated with 100 nM or 25 nM triptolide; 0 h represents untreated baseline levels of caspase-3 activity ($n = 3$, mean \pm SE). Caspase-3 activity was also assessed in $Pkd2^{-/-}$ and $Pkd2^{REX}$ intact cells. Nuclear localized green fluorescence is indicative of active caspase-3. (D) $Pkd1^{-/-}$ cells were treated with 100 nM triptolide or DMSO control over a 96-h time course. Representative fields were photographed under bright field microscopy (10 \times). Cell viability was assessed, and results are graphically represented ($n = 3$, mean \pm SE). PC2 localization in untreated $Pkd1^{-/-}$ cells was visualized by using confocal microscopy (Fluorescein isothiocyanate, 40 \times) and propidium iodide nuclear stain (red). (E) $Pkd1^{-/-}$ cells (starting density of 20×10^5) were cultured in the absence or presence of calcium-containing media \pm 100 nM triptolide for 72 h. Brightfield images show cell density after 72 h of culture, and cell viability following triptolide treatment is graphically represented ($n = 3$, mean \pm SE). (F) Western blot analysis of p21CIP/WAF (Upper) and p53 (Lower) expression in $Pkd1^{-/-}$ cells during a time course of 100-nM triptolide treatment.

expression. Nonconfluent, and therefore nonciliated, $Pkd1^{+/-}$ cells were first examined to determine whether triptolide induces Ca^{2+} release. In this context, PC2 expression would be limited to the ER, where it resides with other calcium channels such as the IP₃R. Upon triptolide addition, we observed a clear rise in intracellular Ca^{2+} levels, which was the first evidence that this small molecule was capable of eliciting Ca^{2+} release in cells (Fig. 3A). Importantly, no Ca^{2+} release was detected upon exposure of these nonciliated cells to buffer flow alone (data not shown). Although activation of one channel can propagate and activate other calcium channels, we wanted to determine specifically whether PC2 and/or PC1 was involved in a calcium-signaling pathway stimulated by triptolide addition. Therefore, we tested the cell lines lacking either PC1 ($Pkd1^{-/-}$) or PC2 ($Pkd2^{-/-}$) (30) expression for this triptolide-mediated calcium response. $Pkd1^{-/-}$ cells responded to triptolide addition with a similar calcium release profile as that of $Pkd1^{+/-}$ cells (Fig. 3B). Interestingly, given the hypothesized regulatory role of PC1 on PC2 function, this biological activity of triptolide was not dependent upon PC1 expression. Because our biochemical purification analysis identified PC2 as a putative triptolide-binding protein, we next assessed whether the observed Ca^{2+} release was dependent upon PC2 expression. When 100 nM triptolide was added to the perfusion solution while examining the response in $Pkd2^{-/-}$ murine kidney epithelial cells, no Ca^{2+} release was detected (Fig. 3C). To strengthen the evidence that PC2 was required for Ca^{2+} release elicited by triptolide addition, $Pkd2^{REX}$ cells were next assessed for sensitivity to triptolide. As shown in Fig. 3D, PC2 reexpression restored triptolide-induced Ca^{2+} release, providing the first mechanistic evidence for triptolide-mediated Ca^{2+} regulation (Fig. 3D). To characterize further the observed calcium response initiated by triptolide, we examined the importance of extracellular calcium in addition to the predominant and well characterized IP₃R and RyR calcium channels. Results from initial

experiments concluded that our murine kidney epithelial cells did not express the RyR because 25 mM of caffeine, a RyR agonist, did not elicit a calcium response. Additionally, $Pkd1^{-/-}$ cells exposed to 50 μM of dantrolene, a RyR antagonist, failed to suppress triptolide-mediated calcium release (data not shown). In contrast, inactivation of the IP₃R with the inhibitor 2APB eliminated any detectable release of calcium upon addition of triptolide (Fig. 3E). Because 2APB has also been reported to block store-operated channels (SOCs) (31), we cannot rule out their possible involvement. Although it is clear that the triptolide-mediated calcium signaling is lost in the absence of PC2, it is also probable that a functional IP₃R is required for the propagation and detection of calcium release in this system. Further evidence implicating an intact interaction of calcium channel-mediated events was shown when triptolide-induced calcium release was inhibited or significantly attenuated in both $Pkd1^{-/-}$ and $Pkd2^{REX}$ cells in Ca^{2+} -free Hank's balanced salt solution (HBSS) (Fig. 3E). Taken together, these data support a model in which triptolide acts in a pathway requiring PC2, but additionally involves the IP₃R and possibly SOCs to fully propagate the calcium signal.

Triptolide Reduces Cystic Burden in a $Pkd1^{-/-}$ Murine Model of ADPKD. Based on the apparent effect of triptolide on growth inhibition and cellular Ca^{2+} release in $Pkd1^{-/-}$ cells, we next sought to determine whether we could alter the course of cyst formation in the $Pkd1^{-/-}$ mouse model of ADPKD. $Pkd1^{-/-}$ animals display midgestational embryonic lethal phenotype due to severe developmental abnormalities (32–34). Kidney and pancreatic cyst formation is evident from E14.5 and E13.5, respectively (33, 35). Triptolide has been previously studied in rodent models of tumor regression (36, 37), but it had not been tested in a system by using pregnant females. To establish first a potential therapeutic and sublethal dosage, pregnant C57BL/6 mice were treated with incre-

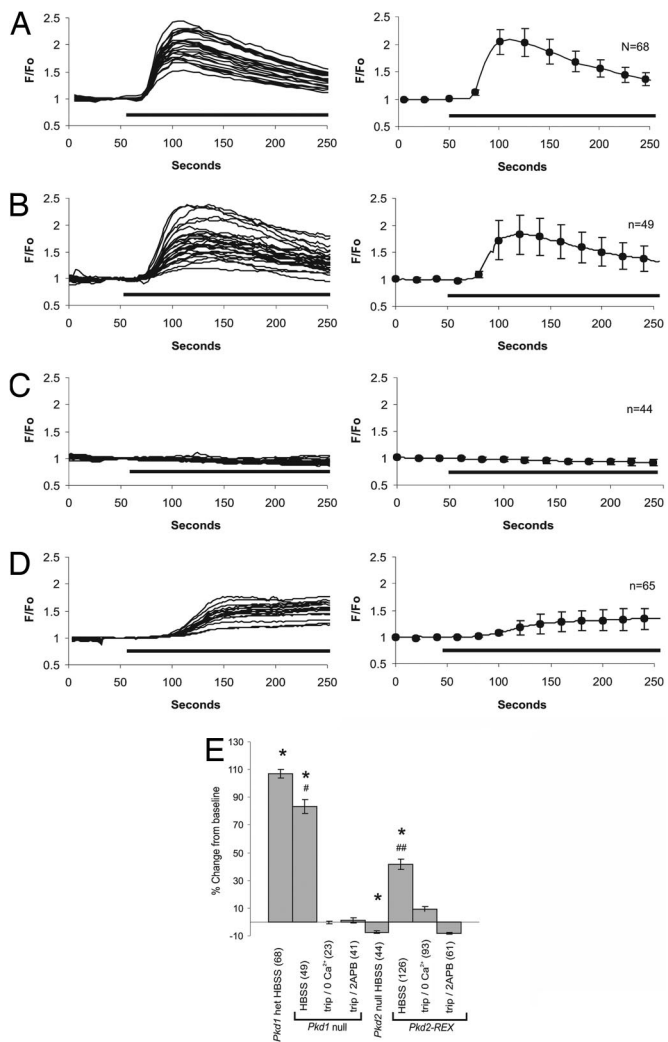


Fig. 3. Triptolide causes a PC2-dependent calcium release in murine kidney epithelial cells. Changes in intracellular calcium levels from *Pkd1*^{+/−} (*A* Left), *Pkd1*^{−/−} (*B* Left), *Pkd2*^{−/−} (*C* Left), and *Pkd2*^{REX} (*D* Left) cells during a typical experiment with 100 nM triptolide (solid bar). The average triptolide response for each genotype is represented on the right side of each panel. (*E*) Average maximum change in intracellular calcium levels elicited by triptolide in *Pkd1*^{+/−}, *Pkd1*^{−/−}, *Pkd2*^{−/−}, and *Pkd2*^{REX} cells in HBSS, Ca²⁺-free HBSS, or in the presence of 200 μM 2APB. Error bars are ± SEM. *, *Pkd1*^{+/−}, *Pkd1*^{−/−}, *Pkd2*^{−/−}, and *Pkd2*^{REX} cells were significantly different from each other, $P < 0.01$; one-way ANOVA, $F = 123.5$, $df = 3$, Tukey multiple comparison test, $P < 0.05$. #, *Pkd1*^{−/−} in HBSS significantly different from Ca²⁺ free and 2APB, $P < 0.01$; one-way ANOVA, $F = 123.5$, $df = 2$, Tukey multiple comparison test; one-way ANOVA, $F = 160.2$, $df = 3$, $P < 0.01$. ##, *Pkd2*^{REX} in HBSS significantly different from Ca²⁺ free and 2APB, $P < 0.01$; one-way ANOVA, $F = 65.9$, $df = 2$, Tukey multiple comparison test.

mental doses of triptolide from 0.01–0.15 mg/kg/day i.p. injections. Toxicity was determined by resorption of all embryos or the preponderance of stillborns. Using this criteria, triptolide toxicity was most prominent at doses of ≥ 0.1 mg/kg/day. However, no discernable adverse effects were observed at 0.07 mg/kg/day, which we thus concluded to be the maximum tolerated dose. Another experimental parameter involved the timing of the start of triptolide injections because PC2 has been shown to be important for left-right axis formation in the developing embryo at approximately E7.75 (38, 39). We therefore chose E10.5 as the start of triptolide injections to allow for normal PC2-mediated development while leaving sufficient time to influence cyst formation during kidney organogenesis.

Following successful *Pkd1*^{+/−} × *Pkd1*^{+/−} intercrosses, 0.07 mg/kg/day of triptolide or DMSO control was injected into pregnant mice from E10.5 until birth. All pups were assessed for multiple parameters, such as genotypic distribution, developmental stage at time of birth, and average kidney weights [supporting information (SI) Table 1]. *Pkd1*^{−/−} mice can be reabsorbed beginning at E12.5, thereby resulting in an atypical Mendelian distribution of *Pkd1*^{−/−} progeny (34, 35). We observed this same reported deviation in expected *Pkd1*^{−/−} numbers, with 20 and 18% for DMSO or triptolide treated, respectively (SI Table 1). Wet weight kidney analysis from *Pkd1*^{+/+} or *Pkd1*^{+/−} mice demonstrated no significant difference in weight or overall size for DMSO or triptolide treated (SI Table 1). *Pkd1*^{−/−} kidneys were larger by weight, although there was no statistically significant difference between DMSO or triptolide treated (17.5 ± 2.0 vs. 21.8 ± 2.8), indicating that the accumulation of fluid in the kidneys was not reduced. Additionally, independent of genotype, triptolide did not have any apparent overall deleterious effect on murine development or length of pregnancy.

Assessment of cyst formation was completed by sagittal cross-sectioning of kidneys, H&E staining, and the calculation of the area of cyst formation as a percentage of total kidney area. Because triptolide is capable of inducing apoptosis or growth arrest, we were concerned that normal kidney development may be adversely affected. This was not the case because *Pkd1*^{+/+} and *Pkd1*^{+/−} kidneys in both treatment groups showed normal morphology where background “cyst values” were calculated to account for random physiological abnormalities or artefacts of tissue handling and preparation (Fig. 4 G–J).

To determine triptolide’s effect on *Pkd1*^{−/−} mice, we next examined kidneys from these animals. *Pkd1*^{−/−} kidneys from animals injected with vehicle alone (DMSO) had a mean cystic burden of $34 \pm 2.7\%$, whereas several had cystic areas between 55–65% of the whole kidney (Fig. 4 A–C and N–O). However, triptolide treatment of *Pkd1*^{−/−} pups resulted in a statistically significant decrease of the cystic burden to an average of $15 \pm 2.1\%$ (Fig. 4 D–F and N). Kidney size varied among litters, from a range of small kidneys with almost no evidence of any cyst formation to a maximum cyst burden of 28% (Fig. 4O). We believe this variability may be due to the proximity of triptolide delivery to the developing fetus during injections. Although the epithelial cells lining the cysts appeared normal by microscopy and the diameter of cyst lumens on average was smaller, we wanted to determine whether the lack of cyst growth due to triptolide treatment was due to the induction of apoptosis or a delay in cell growth. Tissue sections were stained for immunoreactivity toward active caspase-3, a marker of cellular commitment to apoptosis. Both control (Fig. 4L) and triptolide-treated (Fig. 4M) samples did not show any significant activation of the caspase pathway as determined by comparison to secondary antibody control (Fig. 4K).

Discussion

Triptolide has been investigated for many of its potential therapeutic uses, including reduction of solid tumor masses, and is currently in clinical trials based on its potent antitumor effects in a prostate cancer model (20). In this respect, triptolide has been shown repeatedly to induce efficient apoptosis or cell growth arrest depending upon its effective concentration (16). Until now, potential targets of triptolide have not been identified that explain its broad and potent biological effects. Although triptolide does not bind to its target protein(s) covalently (16), we have been able to follow specific [³H]triptolide-binding activity through chromatographic purification to identify PC2 as a putative target protein. Our work here not only demonstrates a correlation between PC2 cellular expression and sensitivity to triptolide-induced growth arrest/cell death, but also reveals for the first time that triptolide causes calcium release through a PC2-dependent pathway.

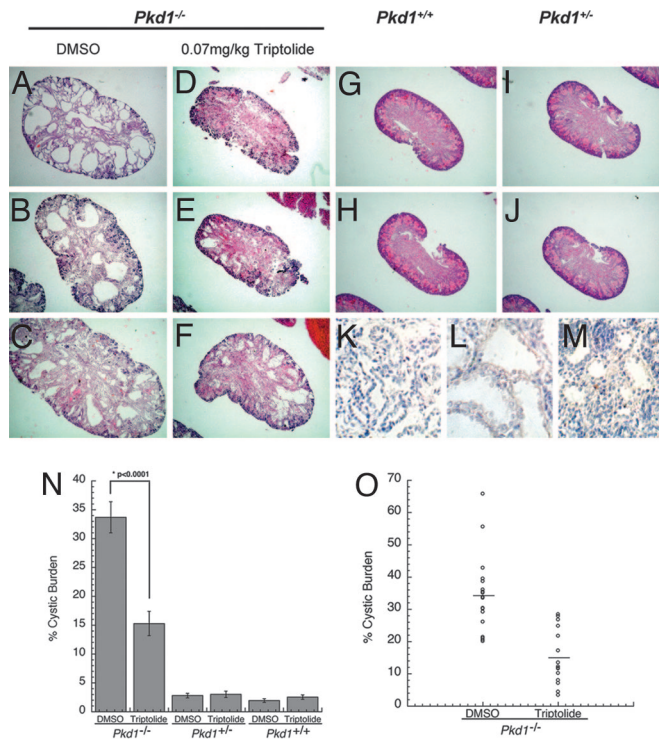


Fig. 4. Triptolide reduces cystic burden in a *Pkd1*^{-/-} murine model of ADPKD. (A–C) Representative kidneys from *Pkd1*^{-/-} pups treated with DMSO during gestation (E10.5–birth). Large cysts are present throughout the medulla and cortex (4 \times magnification). (D–F) Representative kidneys from *Pkd1*^{-/-} pups treated with triptolide during gestation. (G) *Pkd1*^{+/+} kidney from a pup treated with DMSO or (H) triptolide. (I) *Pkd1*^{-/-} kidney treated with DMSO or (J) triptolide. (K–M) IHC staining of *Pkd1*^{-/-} kidneys for active caspase-3 expression: (K) secondary antibody negative control, (L) DMSO treated, and (M) triptolide treated. (N) Percent of cyst burden in the kidney as determined by area in each of the *Pkd1* genotypes (mean \pm SE, *Pkd1*^{-/-}, $n = 18$; *Pkd1*^{+/+}, $n = 10$; and *Pkd1*^{+/+}, $n = 10$). (O) Cystic burden values comparing DMSO or triptolide treatment for each *Pkd1*^{-/-} animal are represented as open circles. The mean value (as shown in N) is represented as a horizontal line.

The discovery that PC2 is required for triptolide-mediated Ca^{2+} release allows us to propose PC2 as an early candidate effector. This conclusion is also supported by our previous findings that triptolide binding and cell death/growth arrest can be modulated by Ca^{2+} concentration (16). Because PC1 has been shown to interact with and regulate PC2 (5, 9, 40–42), our finding that triptolide is able to elicit calcium release in the absence of PC1 expression was of particular interest. However, we cannot rule out the possibility that PC1 may further propagate or sustain triptolide-induced calcium release through PC2. This could potentially explain the observation that, in the absence of PC1 (*Pkd1*^{-/-} cells), triptolide causes growth arrest and p21 up-regulation, but not cell death (Fig. 2). Another interesting finding was the profile of *Pkd2^{REX}* calcium release; during the short course of our imaging experiment, triptolide-induced calcium levels did not return to baseline in these cells (Fig. 3D). It would be of future interest to determine whether this sustained calcium release is responsible for the extreme sensitivity of this cell line to triptolide. Although PC2-null cells failed to release calcium upon triptolide addition, thereby implicating PC2 alone as the mediator for this response, our results also showed that calcium release in PC1-null cells was blocked by inhibition of the IP₃R (Fig. 3E). This finding can possibly be explained by the limit of detection of calcium imaging because the IP₃R is the major calcium channel in the ER and may simply be activated by PC2-stimulated calcium release to propagate fully a signal.

ADPKD cyst formation is similar to benign epithelial neoplasia because both are characterized by abnormal cellular proliferation independent of extracellular cues. Based upon our *in vitro* data showing triptolide-mediated *Pkd1*^{-/-} growth arrest and calcium release, we hypothesized that triptolide could restore calcium signaling and reduce cell proliferation in a *Pkd1*^{-/-} murine model of ADPKD. Indeed we found that triptolide caused a reduction in cyst formation, but did not cause cell death, as assessed by caspase-3 activation (Fig. 4). We did not observe a decrease in fluid secretion, and therefore overall kidney weight, possibly because in the absence of PC1 the chloride channel CFTR remains deregulated (43). Because we were limited in the maximum tolerated dose of triptolide we could administer during gestation, we are hopeful that future studies with higher triptolide concentrations in various adult animal models will prove to be of greater therapeutic benefit.

We have previously found that triptolide's mode of action (i.e., cell growth, cell death, and transcriptional inhibition) can be differentiated by a dependence on calcium (16). Future questions to be answered include the role of PC2 in other cell lines affected by triptolide, such as cancer lines and WBCs. Additionally, it is necessary to understand whether triptolide-induced transcriptional repression is linked to the greater PC2 complex or whether it is through a separate mechanism of action. It would also be of interest to determine whether this PC2-mediated calcium release explains the male antifertility effect of triptolide because PC2 and PC1 have been linked to fertility or male mating behavior in *Drosophila* (44) or *C. elegans* (45, 46). Although we have shown that triptolide induces calcium release in a PC2-dependent pathway, it is also possible that triptolide could cause cell growth arrest through an unrelated or separate mechanism as well. We have previously shown calcium-dependent and -independent effects on triptolide's biological functions, and we acknowledge that, although PC2-null cells are less sensitive to triptolide, they still respond. Agents that act as cell growth inhibitors could and do reduce kidney cyst progression in various disease models as previously demonstrated by the mTOR inhibitor rapamycin (14, 15), a VPV2R antagonist that reduces cAMP levels (13), and by the Cdk inhibitor roscovitine (47). Although triptolide may have multiple modes of action for growth arrest or cell death, this is the first demonstration that a small molecule can specifically cause calcium release through a PC2-dependent pathway. In this regard, triptolide offers a therapeutic strategy of calcium-signaling restoration in the disease state.

In summary, we have identified PC2 as a candidate target for the therapeutic action of the traditional Chinese medicine-derived natural product triptolide, and we propose a pathway to explain triptolide-mediated Ca^{2+} release. Our observation that triptolide arrests *Pkd1*^{-/-} epithelial cell growth and attenuates *in vivo* cyst progression suggests that stimulation of PC2-mediated Ca^{2+} release could serve as a successful clinical ADPKD strategy. Because the natural source of triptolide, the medicinal vine, *Tripterygium wilfordii* Hook F, has a long history in Chinese traditional medicine, it is hoped that triptolide will be a well tolerated, promising therapeutic candidate for the treatment of ADPKD.

Materials and Methods

Cells and Reagents. The *Pkd2*^{-/-} (2D2) murine cell lines were derived as previously reported (30). The *Pkd2^{REX}* cell line was made by stable integration of untagged *Pkd2* under hygromycin selection (30). Antibodies included PC2 (48), cleaved caspase-3 (Cell Signaling Technology, Danvers, MA), p53 (Santa Cruz Biotechnology, Santa Cruz, CA), and p21 (BD Biosciences, San Jose, CA). Triptolide was obtained from Sinobest Inc. (Tongling, Anhui, China), tritiated by Sib Tech, Inc. (Newington, CT), and resuspended in ethanol to a specific activity of 4–6 Ci/mmol (1 Ci = 37 GBq).

Intracellular Ca²⁺ Measurement. Cells were incubated for 30 min with 11 μM Fluo-4 AM (Molecular Probes, Eugene, OR) at 37°C + 0.05% Pluronic F127 in HBSS that contains (in mM) 130 NaCl, 5 KCl, 1 MgSO₄, 1.25 CaCl₂, and 19.7 Hepes (pH 7.4). A Nikon (Tokyo, Japan) TE2000 epifluorescence microscope equipped with a Lambda LS 175W Xenon arc lamp (Sutter Instrument Company, Novata, CA) and a CoolSnap HQ CCD camera (Roper Scientific, Tucson, AZ) was used to visualize the cells. MetaFluor software (Universal Imaging Corporation, Downingtown, PA) was used for data acquisition and analysis. Cells were individually selected, and their fluorescence intensities (F) were normalized with resting fluorescence (Fo) and reported as F/Fo.

In Vivo Murine Experiments. All animal experiments were done in accordance with the Yale Animal Resources Center (YARC) and

Institutional Animal Care and Use Committee (IACUC) regulations. *Pkd1^{+/−} × Pkd1^{+/−}* mice were mated and divided into control (DMSO) or experimental (triptolide) groups. A total volume of 100 μl of PBS with ≤5% DMSO or DMSO/0.07 mg/kg/day triptolide was injected i.p. with a 28G 1/2 insulin syringe. Mice were weighed and injected starting at E10.5 until birth. All pups were examined for length and developmental staging, such as whisker and nail formation. Kidneys were harvested and weighed before fixation. Further details are available in *SI Materials and Methods*.

We thank Barbara Ehrlich for her many helpful conversations and comments on the manuscript. This work was supported by National Institutes of Health Grants AI055914 (to C.M.C.) and DK57328 (to S.S.) and by a postdoctoral fellowship from the American Cancer Society (to S.J.L.).

1. Gabow PA, Grantham JJ (1997) *Polyzystic Kidney Disease* (Little, Brown, Boston).
2. Koulen P, Cai Y, Geng L, Maeda Y, Nishimura S, Witzgall R, Ehrlich BE, Somlo S (2002) *Nat Cell Biol* 4:191–197.
3. Anyatunwu GI, Ehrlich BE (2005) *J Biol Chem* 280:29488–29493.
4. Igarashi P, Somlo S (2002) *J Am Soc Nephrol* 13:2384–2398.
5. Nauli SM, Alenghat FJ, Luo Y, Williams E, Vassilev P, Li X, Elia AE, Lu W, Brown EM, Quinn SJ, et al. (2003) *Nat Genet* 33:129–137.
6. Pazour GJ, Rosenbaum JL (2002) *Trends Cell Biol* 12:551–555.
7. Yoder BK, Hou X, Guay-Woodford LM (2002) *J Am Soc Nephrol* 13:2508–2516.
8. Praetorius HA, Spring KR (2001) *J Membr Biol* 184:71–79.
9. Bhunia AK, Piontek K, Boletta A, Liu L, Qian F, Xu PN, Germino FJ, Germino GG (2002) *Cell* 109:157–168.
10. Li X, Luo Y, Starremans PG, McNamara CA, Pei Y, Zhou J (2005) *Nat Cell Biol* 7:1102–1112.
11. Yamaguchi T, Hempson SJ, Reif GA, Hedge AM, Wallace DP (2006) *J Am Soc Nephrol* 17:178–187.
12. Yamaguchi T, Wallace DP, Magenheimer BS, Hempson SJ, Grantham JJ, Calvet JP (2004) *J Biol Chem* 279:40419–40430.
13. Torres VE, Wang X, Qian Q, Somlo S, Harris PC, Gattone VH, II (2004) *Nat Med* 10:363–364.
14. Shillingford JM, Murcia NS, Larson CH, Low SH, Hedgepeth R, Brown N, Flask CA, Novick AC, Goldfarb DA, Kramer-Zucker A, et al. (2006) *Proc Natl Acad Sci USA* 103:5466–5471.
15. Tao Y, Kim J, Schrier RW, Edelstein CL (2005) *J Am Soc Nephrol* 16:46–51.
16. Leuenroth SJ, Crews CM (2005) *Chem Biol* 12:1259–1268.
17. Kupchan SM, Court WA, Dailey RG, Jr, Gilmore CJ, Bryan RF (1972) *J Am Chem Soc* 94:7194–7195.
18. Lu H, Hachida M, Enosawa S, Li XK, Suzuki S, Koyanagi H (1999) *Transplant Proc* 31:2056–2057.
19. Qiu D, Kao PN (2003) *Drugs R D* 4:1–18.
20. Kiviharju TM, Lecane PS, Sellers RG, Peehl DM (2002) *Clin Cancer Res* 8:2666–2674.
21. Shamon LA, Pezzuto JM, Graves JM, Mehta RR, Wangcharoentrakul S, Sangsuwan R, Chaichana S, Tuchinda P, Cleason P, Reutrakul V (1997) *Cancer Lett* 112:113–117.
22. Wei YS, Adachi I (1991) *Chung Kuo Yao Li Hsueh Pao* 12:406–410.
23. Lee KY, Chang W, Qiu D, Kao PN, Rosen GD (1999) *J Biol Chem* 274:13451–13455.
24. Liu H, Liu ZH, Chen ZH, Yang JW, Li LS (2000) *Acta Pharmacol Sin* 21:782–786.
25. Qiu D, Zhao G, Aoki Y, Shi L, Uyei A, Nazarian S, Ng JC, Kao PN (1999) *J Biol Chem* 274:13443–13450.
26. Carter BZ, Mak DH, Schober WD, McQueen T, Harris D, Estrov Z, Evans RL, Andreff M (2006) *Blood* 108:630–637.
27. Yang Y, Liu Z, Tolosa E, Yang J, Li L (1998) *Immunopharmacology* 40:139–149.
28. Chang WT, Kang JJ, Lee KY, Wei K, Anderson E, Gotmare S, Ross JA, Rosen GD (2001) *J Biol Chem* 276:2221–2227.
29. Jiang XH, Wong BC, Lin MC, Zhu GH, Kung HF, Jiang SH, Yang D, Lam SK (2001) *Oncogene* 20:8009–8018.
30. Grimm DH, Cai Y, Chauvet V, Rajendran V, Zeltner R, Geng L, Avner ED, Sweeney W, Somlo S, Caplan MJ (2003) *J Biol Chem* 278:36786–36793.
31. Prakriya M, Lewis RS (2001) *J Physiol* 536:3–19.
32. Kim K, Drummond I, Ibraghimov-Beskrovny O, Klinger K, Arnaout MA (2000) *Proc Natl Acad Sci USA* 97:1731–1736.
33. Lu W, Peissel B, Babakanlou H, Pavlova A, Geng L, Fan X, Larson C, Brent G, Zhou J (1997) *Nat Genet* 17:179–181.
34. Lu W, Shen X, Pavlova A, Lakkis M, Ward CJ, Pritchard L, Harris PC, Genest DR, Perez-Atayde AR, Zhou J (2001) *Hum Mol Genet* 10:2385–2396.
35. Wu G, Tian X, Nishimura S, Markowitz GS, D'Agati V, Park JH, Yao L, Li L, Geng L, Zhao H, et al. (2002) *Hum Mol Genet* 11:1845–1854.
36. Tengchaisri T, Chawengkirtikul R, Rachaphaew N, Reutrakul V, Sangsuwan R, Sirisinha S (1998) *Cancer Lett* 133:169–175.
37. Yang S, Chen J, Guo Z, Xu XM, Wang L, Pei XF, Yang J, Underhill CB, Zhang L (2003) *Mol Cancer Ther* 2:65–72.
38. McGrath J, Somlo S, Makova S, Tian X, Brueckner M (2003) *Cell* 114:61–73.
39. Pennekamp P, Karcher C, Fischer A, Schweickert A, Skryabin B, Horst J, Blum M, Dworniczak B (2002) *Curr Biol* 12:938–943.
40. Hanaoka K, Qian F, Boletta A, Bhunia AK, Piontek K, Tsikas L, Sukhatme VP, Guggino WB, Germino GG (2000) *Nature* 408:990–994.
41. Tsikas L, Kim E, Arnould T, Sukhatme VP, Walz G (1997) *Proc Natl Acad Sci USA* 94:6965–6970.
42. Xu GM, Gonzalez-Perrett S, Essafi M, Timpanaro GA, Montalbetti N, Arnaout MA, Cantillo HF (2003) *J Biol Chem* 278:1457–1462.
43. Ikeda M, Fong P, Cheng J, Boletta A, Qian F, Zhang XM, Cai H, Germino GG, Guggino WB (2006) *Cell Physiol Biochem* 18:9–20.
44. Watnick TJ, Jin Y, Matunis E, Kernan MJ, Montell C (2003) *Curr Biol* 13:2179–2184.
45. Barr MM, DeModena J, Braun D, Nguyen CQ, Hall DH, Sternberg PW (2001) *Curr Biol* 11:1341–1346.
46. Barr MM, Sternberg PW (1999) *Nature* 401:386–389.
47. Bukanov NO, Smith LA, Klinger KW, Ledbetter SR, Ibraghimov-Beskrovny O (2006) *Nature* 444:949–952.
48. Cai Y, Maeda Y, Cedzich A, Torres VE, Wu G, Hayashi T, Mochizuki T, Park JH, Witzgall R, Somlo S (1999) *J Biol Chem* 274:28557–28565.